Solar Energy Materials & Solar Cells 133 (2015) 113–118

Contents lists available at ScienceDirect

Solar Energy Materials & Solar Cells

journal homepage: www.elsevier.com/locate/solmat

Accurate extraction of the series resistance of aluminum local back surface field silicon wafer solar cells

Jia Chen [a,b,*], Zhe Ren Du [a,c], Fajun Ma [a,c], Fen Lin [a], Debajyoti Sarangi [a], Bram Hoex [a], Armin G. Aberle [a,b,c]

[a] Solar Energy Research Institute of Singapore, National University of Singapore, Singapore
[b] NUS Graduate School for Integrative Sciences and Engineering, National University of Singapore, Singapore
[c] Department of Electrical and Computer Engineering, National University of Singapore, Singapore

ARTICLE INFO

Article history:
Received 7 April 2014
Received in revised form
20 August 2014
Accepted 3 October 2014

Keywords:
Al-LBSF
Silicon solar cells
Series resistance

ABSTRACT

Aluminum local back surface field (Al-LBSF) silicon wafer solar cells are currently intensively investigated in the photovoltaic community and are expected to enter mass production in the near future. In this work we show that this solar cell architecture can pose significant challenges in the determination of the series resistance at the maximum power point. We also show that some of the traditional methods for extracting the series resistance of these cells result in a severe underestimation, due to injection dependent saturation current densities. By using a combination of electro- and photo-luminescence images, we demonstrate that the series resistance of Al-LBSF solar cells can be accurately determined.

1. Introduction

The silicon (Si) wafer based sector of the photovoltaic (PV) industry is trying to reduce costs by increasing the solar cell efficiency of increasingly thinner Si wafers. A standard full-area Al back surface field (Al-BSF) provides only a moderate level of electronic passivation of the rear surface. With significantly improved rear passivation at a relatively low additional cost, solar cells with an Al local back surface field (Al-LBSF) [1] are of great interest. However several issues were observed for screen-printed Al-LBSF solar cells, such as thin p^+ layers within the rear contacted regions [2] and the formation of voids between the Si substrate and the Al rear contact [3,4]. A large series resistance R_s can be observed for this type of solar cell due to the fact that the majority charge carriers need to travel laterally to the rear electrode for collection and, in addition, the contact resistance at the rear is generally higher compared to a full-area Al back surface field (Al-BSF) [5].

Therefore, it is important to accurately extract R_s to characterize and improve the efficiency of Al-LBSF solar cells. Due to the distributed nature of R_s [6–8] it is a function of both voltage and current [9,10]. The current path within the emitter alters when the external conditions change. The R_s of a solar cell can thus be significantly different in dark or under illumination [11]. The series resistance at standard operating condition, $R_{s,lightMPP}$, is the most important parameter to consider as this quantifies the effect of R_s on the solar cell efficiency. The standard operating condition for a terrestrial solar cell refers to the maximum power point (MPP) under AM1.5G illumination at 25 °C cell temperature. The use of $R_{s,lightMPP}$ in advanced fill factor [12] and power loss analyses [13] is also helpful for identifying fabrication issues and improving the efficiency of Al-LBSF solar cells.

In this work, multicrystalline Al-LBSF solar cells were fabricated and their $R_{s,lightMPP}$ was determined using conventional methods [14]: comparison of dark and 1-Sun light I–V measurements (DIV–LIV method) [10], comparison of one-Sun light I–V and J_{sc}–V_{oc} measurements (J_{sc}–V_{oc} method) [10,15], fill factor method [16], and a combination of electro- and photo-luminescence imaging measurements ($R_{s\text{-}PL}$ method) [17]. The comparison of light I–V curves under different illumination levels (double-light method) [15] was not available in this work due to limitations of our I–V tester. We observed a significant underestimation of $R_{s,lightMPP}$ (due to the strongly injection level dependent saturation current densities J_{01} and J_{02}) for the DIV–LIV and J_{sc}–V_{oc} methods. We show that $R_{s,lightMPP}$ can be extracted accurately with the $R_{s\text{-}PL}$ method, as this method extracts $R_{s,lightMPP}$ under operating conditions with a constant bulk injection level. From two-diode simulations and a detailed analysis, it seems that this result is valid not only for Al-LBSF cells but also for other types of solar cells.

2. Experimental setup

A batch of p-type 6 in. wide multicrystalline silicon Al-LBSF solar cells with homogenous n-type emitter was fabricated

---

* Corresponding author at: Solar Energy Research Institute of Singapore, National University of Singapore, 7 Engineering Drive 1, Block E3A, #06-01, Singapore 117574, Singapore. Tel.: +65 66011677.
E-mail address: a0033548@nus.edu.sg (J. Chen).

http://dx.doi.org/10.1016/j.solmat.2014.10.003
0927-0248/© 2014 Elsevier B.V. All rights reserved.

according to the processing flow of Fig. 1. The wafers were wet-chemically textured on both sides, followed by a phosphorus diffusion of 70 Ω/sq. After wet-chemical edge isolation and phosphosilicate glass (PSG) removal, a 100 nm thick masking layer of silicon nitride (SiN_x) was deposited onto the front surface by plasma-enhanced chemical vapor deposition (PECVD). A chemical solution ('SERIS etch' [18]) developed in our institute was used for rear side polishing. The wafers were then split into three groups. The masking layer of Group C was removed by etching in diluted HF (10%), and a 70 nm SiN_x antireflection coating was deposited onto the front of the wafers. A stack of 40 nm aluminum oxide (AlO_x) and 100 nm SiN_x was then deposited onto the rear of the wafers of all groups. All the dielectric layers were deposited by PECVD in an industrial inline deposition system (SiNA-XS, Roth & Rau). All groups were completed into full solar cells with optimized laser-opened line contacts (100 µm wide lines with a pitch of 1.0 mm [19–21]). For the laser processing step, a laser with picosecond pulses (duration ~10 ps, wavelength 532 nm) was used (Super Rapid, Lumera). Solar cells of Group A received a short KOH dip (10%, 70 °C) after laser ablation to remove possible laser damage [19]. Cells from all groups were then fired in an industrial belt fast firing furnace (Ultraflex, Despatch Industries) with a set peak temperature of 800 °C. For reference purposes, standard full-area Al-BSF solar cells were also fabricated in this experiment. Upon completion of all solar cells, the 1-Sun and dark current–voltage characteristics were measured under standard testing conditions (Solsim 210, Aescusoft). The solar cells were also analyzed with the Suns–V_{oc} method (Sinton, WCT-120).

From the measured data, $R_{s,lightMPP}$ was determined using the DIV–LIV, J_{sc}–V_{oc}, and FF methods. The $R_{s,lightMPP}$ was also extracted from a combination of electro- and photo-luminescence imaging measurements (LIS-R1, BT Imaging) [17]. One cell from every group was selected for a detailed analysis of the measured I–V characteristics using the two-diode model. Finally the effective minority carrier lifetime τ_{eff} of the solar cells was extracted from Suns–V_{oc} measurements (Suns–V_{oc}, Sinton Instruments).

3. Experimental results and discussion

3.1. Solar cell results

The measured 1-Sun I–V parameters of the investigated multi-Si Al-LBSF solar cells are listed in Table 1. Two cells from each group were selected for investigation. Cells from Group C have a higher open-circuit voltage (V_{oc}), fill factor (FF) and efficiency (eff) due to their better front surface passivation. The front SiN_x of Group A and Group B cells deteriorated during the step of rear side polishing and KOH etching. The $R_{s,lightMPP}$ of several representative cells from each group was determined using the DIV–LIV, J_{sc}–V_{oc}, FF and $R_{S\text{-}PL}$ methods Fig. 2. The $R_{s,lightMPP}$ of the Al-BSF reference cells fabricated in the same batch was determined to be ~0.50 ± 0.01 Ω cm^2, using the DIV–LIV method. Compared to Al-BSF cells, there is an additional series resistance ΔR_s for Al-LBSF cells with an identical front grid, emitter and bulk resistivity. This ΔR_s is due to lateral transport of carriers in the bulk and an increased contact resistance [5,22]. Based on the Fischer–Plagwitz model [5,22], ΔR_s of our LBSF cells is 0.15 Ω cm^2. The lower limit of $R_{s,lightMPP}$ of our Al-LBSF cells is thus about 0.65 Ω cm^2. As can be seen from Fig. 2 the J_{sc}–V_{oc} method and, particularly, the DIV–LIV method produce a severe underestimation of $R_{s,lightMPP}$ of Al-LBSF cells of Groups A and B. In contrast, for Group C cells all 4 R_s methods are found to give rather consistent results.

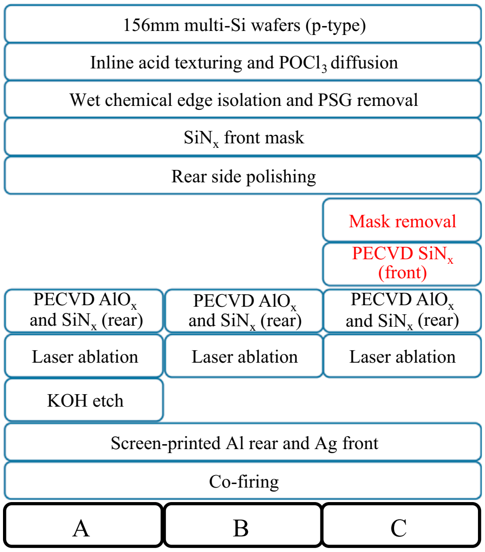

Fig. 1. Fabrication sequence of the investigated Al-LBSF solar cells. The peak temperature during the co-firing step was 800 °C.

3.2. Comparison of different methods for R_s determination

To investigate the differences between the $R_{s,lightMPP}$ values determined by the different methods, we need to discuss these methods and their boundary conditions in more detail. In the DIV–LIV method, the J_{sc}-shifted 1-Sun light (LIV) and dark I–V curves (DIV) are compared. Assuming constant saturation current densities, and negligible impact of both the shunt and the series resistance in the dark [10], the voltage difference ($\Delta V_{\text{DIV–LIV}}$) between these two curves at J_{MPP} can be solely attributed to the 1-Sun series resistance. Using the current at MPP (J_{MPP}), $R_{s,lightMPP}$ at the MPP can be calculated by

$$R_{s,\text{DIV}-\text{LIV}} = \Delta V_{\text{DIV}-\text{LIV}} / J_{MPP} \qquad (1)$$

The J_{sc}–V_{oc} method is not affected by the impact of the series resistance, as neither J_{sc} nor V_{oc} of reasonably good Si wafer solar

Table 1
Measured one-Sun parameters of the investigated Al-LBSF cells. Two cells from each group were selected.

Cell parameter	Group A		Group B		Group C	
	A1	A2	B1	B2	C1	C2
J_{sc}[mA/cm^2]	35.3	34.9	35.2	35.3	35.6	35.5
V_{oc}[mV]	608	560	608	607	620	620
FF [%]	74.1	69.1	72.3	73.2	76.2	77.2
eff [%]	15.9	13.5	15.5	15.6	16.8	17.0

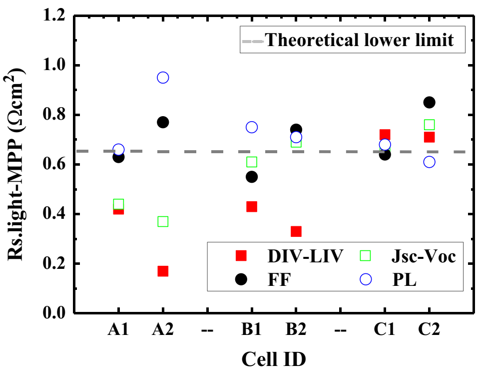

Fig. 2. $R_{s,lightMPP}$ of selected Al-LBSF cells as determined by the DIV–LIV, J_{sc}–V_{oc}, FF and $R_{S\text{-}PL}$ methods. The dashed line is the theoretical lower limit of the Al-LBSF cells expected from the Al-BSF reference cells and the Fischer–Plagwitz model.